JOURNAL PRE-PROOF

This is an early version of the article, published prior to copyediting, typesetting, and editorial correction. The manuscript has been accepted for publication and is now available online to ensure early dissemination, author visibility, and citation tracking prior to the formal issue publication.

It has not undergone final language verification, formatting, or technical editing by the journal's editorial team. Content is subject to change in the final Version of Record.

To differentiate this version, it is marked as "PRE-PROOF PUBLICATION" and should be cited with the provided DOI. A visible watermark on each page indicates its preliminary status.

The final version will appear in a regular issue of *Engineering Transactions*, with final metadata, layout, and pagination.

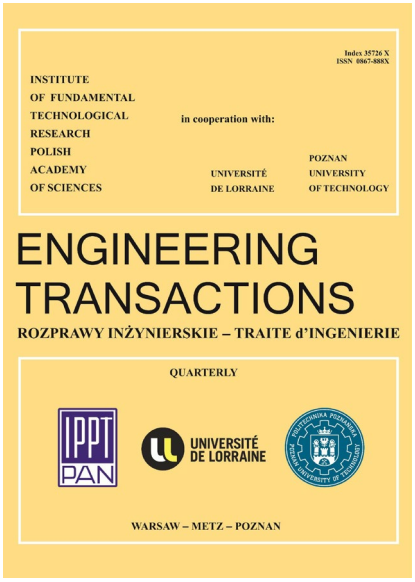

Title: Multi-objective Collaborative Optimization of Steel Structure Central Support Components Integrating NSGA-II and Topology Optimization

Author(s): Lei Han, Heng Zheng, Jianying Weng, Xue Li

DOI: https://doi.org/10.24423/engtrans.2026.3635

Journal: *Engineering Transactions*

ISSN: 0867-888X, e-ISSN: 2450-8071

Publication status: In press

Received: 2025-08-06

Revised: 2026-02-25

Accepted: 2026-03-14

Published pre-proof: 2026-05-11

Please cite this article as:

Han L., Zheng H., Weng J., Li X., Multi-objective Collaborative Optimization of Steel Structure Central Support Components Integrating NSGA-II and Topology Optimization, *Engineering Transactions*, 2026, https://doi.org/10.24423/engtrans.2026.3635

Multi-objective Collaborative Optimization of Steel Structure Central Support Components Integrating NSGA-II and Topology Optimization

Lei Han[1], Heng Zheng[2 *], Jianying Weng[1], Xue Li[1]

[1]School of Engineering, Shandong University of Engineering and Vocational Technology, Jinan, 250200, China

[2] School of Civil Engineering, Shandong Polytechnic, Jinan, 250104, China

[*]Corresponding author email: zhengh8090@outlook.com

Abstract: This paper presents a multi-objective collaborative optimization framework for central support components in steel structures, aiming to simultaneously minimize structural mass and compliance. Traditional design methods often optimize a single objective, limiting overall performance. To address this, we integrate the NSGA-II genetic algorithm with the SIMP topology optimization method within a master-sub nested architecture. NSGA-II performs a global search for optimal macro-level geometric parameters, while SIMP optimizes the micro-level material distribution under given geometries. The interaction between both levels enables a comprehensive trade-off between lightweight design and structural stiffness. Case studies on various support types demonstrate that the proposed method effectively reduces structural mass while enhancing stiffness, confirming its robustness and broad applicability. The Pareto front achieves a high Hypervolume (HV) index, indicating excellent solution diversity and quality. This approach provides an intelligent and efficient pathway for the high-performance, lightweight design of steel structures.

Keywords: Steel Structure, Central Support Member, Multi-objective Optimization, Topology Optimization, NSGA-II Algorithm, Collaborative Optimization

1. Introduction

1.1 Research Background and Significance

Steel structures are widely utilized in modern construction, including high-rise buildings, large-span spatial structures, and industrial plants, owing to their high strength-to-weight ratio, ductility, and recyclability [1]. In particular, Q345 steel offers a yield strength of 345 MPa with a material density of 7.85 g/cm³, making it suitable for load-bearing and seismic-resistant systems. The central support member, as a critical element in steel frame lateral force-resisting systems, considerably enhances structural stiffness and load capacity when properly configured [2–3]. Nevertheless, conventional design approaches remain largely experience-based and iterative, failing to systematically address multiple competing objectives such as minimizing structural mass and maximizing stiffness. Single-objective optimization—for example, minimizing mass alone—often leads to a considerable increase in structural compliance (by 20%–35%), making it challenging to satisfy deformation limits under modern design codes such as GB50017-2017 [4–5]. Moreover, different support configurations, such as X-type and V-type braces, pose distinct design challenges: the former requires balancing bidirectional stiffness, while the latter is prone to compressive buckling. Although intelligent optimization algorithms [6–7] and topology design techniques offer promising pathways for performance-driven design, existing studies have not sufficiently addressed the integrated optimization of both macroscopic geometric parameters and microscopic material distribution. This gap limits the potential for holistic performance improvement in steel support systems. Therefore, this study undertakes multi-objective optimization of central support components [8–9], aiming not only to enhance structural safety and economy but also to promote sustainable and intelligent design practices in steel construction.

1.2 Research Contribution and Innovation

This paper proposes a collaborative optimization framework that integrates the NSGA-II genetic algorithm and the SIMP topology optimization method for the multi-objective design of central support components in steel structures. The primary innovation lies in the establishment of a master-sub nested architecture that enables simultaneous optimization at both macro (geometric parameters) and micro (material distribution) scales—a challenging task due to the inherent differences in search mechanisms and variable types between population-based evolutionary algorithms and gradient-driven topology optimization. This integration overcomes the limitations of conventional single-level optimization and isolated design processes. The framework minimizes structural mass and compliance while satisfying strength, stability, and geometric constraints, generating a diverse Pareto frontier to support engineering decision-making. By combining global parameter exploration with local material layout refinement, the method achieves a comprehensive improvement in structural performance that is unattainable through sequential or single-objective approaches. Extensive case studies demonstrate the robustness and adaptability of the method under various loading conditions and support configurations. The expected practical benefits include significant material savings, enhanced structural efficiency, and a streamlined design process for intelligent and lightweight steel structures, offering a generalizable technical framework that bridges the gap between computational optimization and engineering application.

2. Related Work

In recent years, genetic algorithms have been widely used in the field of structural optimization, especially in solving complex nonlinear optimization problems, showing strong global search capabilities [10-11]. NSGA-II [12-13], as a classic multi-objective genetic algorithm, has achieved efficient Pareto frontier approximation in engineering optimization by applying fast non-dominated sorting and crowding distance mechanisms. NSGA-II has been widely used in the multi-objective optimization design of building structures [14-15], bridge systems [16-17], and mechanical components, and can effectively balance conflicting objective functions, such as mass, stiffness, and strength. Early studies mainly used single-objective methods such as genetic algorithms and particle swarm optimization to optimize the geometric parameters of supporting components. Although such methods can improve local efficiency, they cannot take into account conflicting objectives such as stiffness and stability. The optimization research of steel structure support components has evolved from single-objective parameter optimization to multi-objective collaborative optimization. To balance the multi-objective conflicts, NSGA-II [18-19] can provide a set of compromise solutions, facilitating engineers to make decisions based on actual needs. In addition, its combination with finite element analysis tools further improves the automation level and engineering applicability of structural optimization [20]. Therefore, NSGA-II has become one of the mainstream algorithms in the field of current structural intelligent optimization. However, traditional multi-objective optimization relies on manual decision-making to select Pareto solutions and lacks an automatic matching mechanism with engineering standards.

As an important means of structural lightweight design, topology optimization aims to reasonably distribute materials within a given design domain to achieve optimal performance. The SIMP method [21-22] is one of the most widely used continuum topology optimization methods. It applies pseudo-density variables to interpolate material properties and uses penalty factors to suppress intermediate density, thereby obtaining a clear material distribution. The SIMP method [23-24] is usually combined with finite element analysis to iteratively update the material distribution based on sensitivity information, and finally converge to the optimal

configuration that satisfies the objective function and constraints. SIMP has been widely used in aerospace, automobile manufacturing, construction engineering, and other fields, especially for improving component-level structural performance and optimizing material utilization efficiency [25]. Although the SIMP method has advantages in mathematical modeling and calculation accuracy, its sensitivity to initial conditions and its tendency to fall into local optimality still need to be improved by combining with intelligent optimization strategies. Existing studies are mostly aimed at homogeneous materials, and no density update strategy is optimized for specific stress concentration of X-type and K-type supports.

As a key component of the steel frame lateral force resistance system, the geometric form, cross-sectional size, and material distribution of the central support member directly affect the bearing capacity and stability of the overall structure [26-27]. Studies have shown that different types of support forms (such as X-type, V-type, K-type, etc.) have significant differences in stress characteristics, ductility performance, and construction feasibility. Therefore, the reasonable selection and optimization design of support members are crucial to improving structural performance [28]. Traditional design methods mainly rely on empirical judgment and repeated trial and error, which makes it difficult to meet safety requirements while taking into account economic efficiency [29]. In recent years, with the development of computational mechanics and intelligent optimization technology, an increasing number of studies have begun to combine multi-objective optimization algorithms [30-31] with finite element analysis [32] for cross-section optimization, layout optimization, and morphological evolution of support components. However, existing research focuses on the macroscopic parameter level, and rarely involves the collaborative optimization of the microscopic material distribution level. Although significant progress has been made in macro parameter optimization and micro topology optimization in their respective fields [33-34], research on effectively integrating the two is still relatively limited and faces many challenges. The existing attempts can be mainly divided into two categories: one is to adopt sequential optimization strategy, which first determines the optimal geometric parameters through genetic algorithm, and then performs topology optimization under a fixed configuration. This method ignores the coupling effect between levels and is prone to falling into local optima; The second is to embed the sensitivity information of topology optimization into evolutionary algorithms, but there is often a contradiction between computational efficiency and convergence when dealing with mixed problems of discrete and continuous variables [35]. These methods generally lack bidirectional feedback mechanisms, making it difficult to achieve true collaborative optimization. The NSGA-II and SIMP master-slave nested architecture proposed in this article overcomes the limitations of traditional one-way data streams by establishing a closed-loop interaction between macroscopic parameter space exploration and microscopic material distribution updates, providing a new approach for achieving full-scale performance optimization of steel structure support systems. On this basis, this paper proposes a multi-objective collaborative optimization model that integrates NSGA-II and SIMP methods to achieve the joint optimization design of central support components at the two levels of geometry and material distribution, providing a new technical path for improving structural performance.

3. Method

3.1 Problem Definition and Objective Function

This study aims to construct a multi-objective optimization model that integrates the NSGA-II genetic algorithm and the SIMP topology optimization method to optimize the parameter configuration design of the central support components of the steel structure.

In this optimization problem, the core goal is to achieve the dual optimization goals of minimizing mass and flexibility by adjusting the geometric parameters and material distribution of the support components, thereby improving the mechanical properties and material utilization efficiency of the overall structure while meeting the constraints of structural safety and stability.

Mass is an important indicator to measure the economic efficiency and lightweight degree of a structure. Under the premise of meeting the requirements of bearing capacity and stiffness, reducing mass helps to reduce material costs, mitigate seismic response, and improve construction efficiency. The formula for structural mass is:

$$f_1(x)=M(x)=\sum_e \rho_e V_e \quad (1)$$

In formula (1), x is the design variable vector, including the geometric parameters and material distribution density of the supporting member; ρ_e is the material density of the e-th unit; and V_e is the volume of the e-th unit.

Flexibility is an important indicator to measure the overall deformation capacity of a structure under external loads. Its physical meaning is the strain energy of the structure under load. The smaller the flexibility, the higher the structural rigidity, the smaller the deformation, and the stronger the overall bearing capacity and lateral stiffness of the structure. The formula for flexibility is:

$$f_2(x)=U(x)=\frac{1}{2}F^T K^{-1} F \quad (2)$$

In formula (2), F is the external load vector; K is the overall stiffness matrix of the structure; K^{-1} is the inverse of the stiffness matrix and represents the flexibility matrix of the structure; and $F^T K^{-1}$ is the energy coupling between load and displacement.

Since there is a nonlinear and non-monotonic trade-off between mass and flexibility, that is, reducing mass may lead to a decrease in structural stiffness, while increasing stiffness usually comes at the expense of increasing mass, this study uses a multi-objective optimization method for collaborative optimization. The formula is:

$$\text{Minimize} f_1(\mathrm{x}) = M(\mathrm{x}) = \sum_{e=1}^{E} \rho_e \rho_{\mathrm{mat}} V_e \quad (3)$$

$$\text{Minimize} f_2(\mathrm{x}) = U(\mathrm{x}) = \frac{1}{2}\mathrm{F}^T \mathrm{K}(\mathrm{x})^{-1}\mathrm{F} \quad (4)$$

In formula 3-4, ρ_{mat} is the material density, V_e is the unit volume, F is the external load vector, and K (x) is the overall stiffness matrix that depends on the design variables.

$$\begin{cases} g_j(x)\le 0, j=1,2,\cdots,m \\ \mathrm{h}_k(x)=0,\ k=1,2,\cdots,n \\ x^L \le x \le x^U \end{cases} \quad (5)$$

In formula (5), $g_j(x)$ is the inequality constraint, including strength, stability, and geometric restrictions; $\mathrm{h}_k(x)$ is the equality constraint, including boundary conditions and symmetry requirements; x^L and x^U are the lower and upper limits of the design variables, respectively.

In practical engineering, minimizing quality is directly related to material costs and construction convenience. As a measure of structural strain energy, the minimization of flexibility is closely related to structural performance: lower flexibility values directly correspond to higher overall stiffness, which means that structural deformation is smaller under the same load; The increase in stiffness further enhances the load-bearing capacity of the structure, especially when subjected to wind and earthquake loads, which can effectively control lateral displacement; In addition, according to the Code for Seismic Design of Buildings (GB50011-2010), controlling structural deformation is one of the key factors to ensure seismic performance. Therefore, optimizing flexibility directly

helps to meet the displacement limit requirements in seismic design. This study achieved the optimal balance between material economy and structural performance by jointly optimizing these two objectives while ensuring structural safety and applicability.

3.2 Design Variable Selection

This study adopts a multi-scale collaborative optimization strategy and divides the design variables into two levels: macro variables and micro variables, which are controlled by the NSGA-II genetic algorithm and the SIMP topology optimization method, respectively, thereby achieving the joint design of geometric parameter optimization and material distribution optimization.

Macro-design variables mainly describe the geometric configuration information of the support components in the overall structure, including the support layout angle, cross-sectional dimensions, number of supports, and support positions. These variables determine the force path and bearing capacity of the support components in the structural system and are important parameters that affect the overall performance of the structure.

Support arrangement angle (θ): The angle between the support rod and the horizontal direction, which affects the load transfer path and the stress state of the component, and the value range is $30°\leq\theta\leq60°$;

Cross-sectional size (A): Expressed as the cross-sectional area parameter of the steel section, it affects the bearing capacity and stiffness of the component;

Number of supports (n): The number of support rods, which affects the overall lateral stiffness and redundancy;

Support position (x, y): The arrangement position of the support component in the structural plane, which affects the symmetry and force balance of the structure.

The NSGA-II algorithm is used for global search and optimization, and the macro design variable vector is expressed as:

$$x_{macro}=[\theta,A,n,x,y]^T \quad (6)$$

The micro-design variable describes the material distribution state inside the supporting component and is used to control the distribution density of the material in the design domain. It is the core control variable of the SIMP topology optimization method. This variable is expressed as pseudo-density (ρ_e), and its physical meaning is the relative density of the material in the e-th finite element unit, with a value range of $0 \leq \rho_e \leq 1$.

$\rho_e=0$: It indicates that the unit has no material, that is, it is a void;

$\rho_e=1$: It indicates that the unit is solid material;

$0<\rho_e<1$: It indicates an intermediate density state, which is suppressed by a penalty factor to obtain a clear topological configuration.

In the SIMP method, the relationship between the unit stiffness matrix and the material density is:

$$K_e(\rho_e)=\rho_e^p K_e^0 \quad (7)$$

In formula (7), K_e^0 is the unit stiffness matrix of the solid material; p is the penalty factor, and its value is p=3, used to suppress the intermediate density and obtain a clear material distribution.

The micro-design variable vector is expressed as:

$$x_{micro}=[\rho_1,\rho_2,\ldots,\rho_E]^T \quad (8)$$

Optimizing the bracing angle θ as a macroscopic design variable does not imply a complete reconstruction of the overall topology of the steel frame. In practical engineering, the beam-column layout of the frame is usually predetermined by the building's functional requirements, and the bracing arrangement needs to be carried out within this established frame. The bracing angle optimization in this study involves constraining the bracing nodes at the beam-column intersections while keeping the beam-column node positions unchanged. By adjusting the angle between the bracing members and the horizontal direction, the optimal force transmission angle is found within a continuous range ($30° \leqslant \theta \leqslant 60°$). This approach is equivalent to parametrically optimizing the bracing arrangement within a given frame grid, rather than changing the frame's geometric topology, thus possessing clear engineering feasibility.

3.3 Constraint Modeling

If the optimization model does not consider the actual engineering constraints, it may generate a physically infeasible or constructively infeasible structural form. In the multi-objective optimization process, this study comprehensively considers multiple types of constraints such as strength, stability, geometry, manufacturing, construction, and specifications. It constructs a constraint modeling system for engineering applications to ensure that the optimization results have good safety and feasibility while meeting the performance goals.

Strength constraints are used to ensure that the stress of each unit does not exceed the yield strength of the material under the design load to prevent plastic damage or local failure. For the central support member of the steel structure, the strength constraint is expressed as:

$$\sigma_e \leq f_y, \forall e \quad (9)$$

In formula (9), σ_e is the equivalent stress of the e-th unit; f_y is the yield strength of the steel; and e is the finite element unit index.

Stability constraints are used to prevent buckling failure of support members under compression and are the core control conditions in the design of central support structures. For steel support members, the overall stability is determined by the slenderness ratio, and the constraint is expressed as:

$$\lambda = \frac{l_0}{i} \leq \lambda_{max} \quad (10)$$

In formula (10), l_0 is the calculated length of the member; i is the section radius of gyration; λ_{max} is the maximum slenderness ratio allowed by the code. The *Code for Design of Steel Structures* GB50017 stipulates the slenderness ratio limit of the central support member.

Geometric constraints are used to control the layout and size range of supporting components in the structural system to ensure that the optimization results meet the design intent and construction requirements. The layout range of supporting components should be limited to the area allowed by the structural lateral force resistance system to avoid conflicts with the main beam-column nodes or affecting the building function. To prevent the structure from being too small, resulting in construction difficulties or insufficient bearing capacity, set the minimum component size constraint:

$$A_e \geq A_{min}, \forall e \quad (11)$$

In formula (11), A_{min} is the minimum cross-sectional area.

Avoid slender components and isolated holes: Slender components are prone to local buckling, and isolated holes may weaken the integrity of the structure. Therefore, density filtering technology and minimum size constraints are applied in topology optimization to suppress unreasonable material distribution;

Control the number of connection nodes: Too many connection nodes can increase the difficulty and cost of construction. Therefore, during the optimization process, the number of connection nodes between supporting members and beams and columns should be limited to ensure a simple structure and easy construction.

Code constraints are key constraints that ensure that the optimized structure complies with national or industry design standards. Based on the *Code for Design of Steel Structures (GB50017-2017)* and *the Code for Seismic Design of Buildings (GB50011-2010)*, this study verifies the compliance of the selection of supporting components, mechanical performance, ductility requirements, and node construction to ensure that the optimized structure has sufficient safety and reliability within its design service life.

3.4 Model Coupling Mechanism Design

To achieve the joint optimization design of the central support components of steel structures at two levels of geometric parameters and material distribution, this study proposes a collaborative optimization model based on the NSGA-II and SIMP methods. NSGA-II is used as the main optimizer to perform global search in the macro parameter space, while SIMP is used as a sub-optimizer to optimize the micro material distribution under given geometric parameters, forming a master-sub nested optimization architecture.

The collaborative optimization model based on NSGA-II and SIMP method is shown in Figure 1.

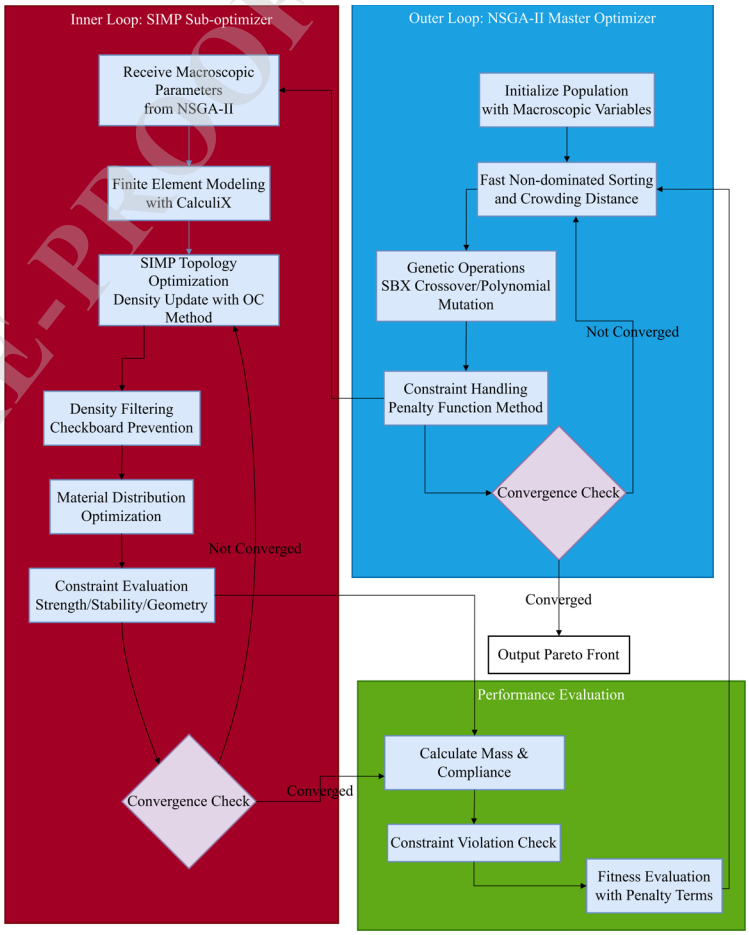

Figure 1. Collaborative optimization model

The collaborative optimization model based on NSGA-II and SIMP methods proposed in this article adopts a master-slave nested double-layer architecture to achieve joint optimization design of steel structure center support components at two levels: geometric parameters and material distribution. The outer NSGA-II algorithm serves as the main optimizer, responsible for conducting global searches in macro parameter spaces such as support angles, cross-sectional dimensions, and layout positions. It generates Pareto frontiers through non dominated sorting and crowding distance mechanisms; The inner layer SIMP method serves as a sub optimizer to perform topological optimization on the micro material distribution under given geometric parameters. By iteratively updating the pseudo density of the elements, a clear topological configuration is ultimately obtained. The coupling between the two layers is achieved through an automated data interface: the geometric parameters generated by NSGA-II drive finite element modeling, and the material distribution feedback quality and flexibility values optimized by SIMP are used for fitness evaluation. This model strictly follows constraints such as strength, stability, and geometric feasibility, and applies density filtering technology to ensure manufacturing feasibility, thus constructing an efficient, stable, and engineering applicable collaborative optimization framework.

The determination of load values within the SIMP topology optimization design domain is based on overall structural analysis. First, the various loads (dead load, live load, wind load, seismic action) and their combinations acting on the overall frame are determined. Under the current macroscopic geometric parameters (support inclination angle, cross-sectional dimensions, etc.) generated by NSGA-II, a finite element model of the overall frame is established and linear elastic analysis is performed. From the analysis results, the axial force design value of the support member to be optimized under the control condition (usually the most unfavorable load combination under the ultimate limit state) is extracted. This axial force value is the external load input for the SIMP sub-optimization problem, acting on the boundary of the topology optimization design domain in the form of concentrated forces or equivalent uniformly distributed forces. This method ensures that the load conditions upon which the microscopic material distribution optimization is based truly reflect the actual stress state of the support member in the overall structure, realizing a closed-loop load transfer from system-level analysis to component-level optimization.

3.5 Algorithm Implementation Details

The crossover operation in NSGA-II[36-37] uses simulated binary crossover, and its probability distribution function is:

$$P_{\mathrm{SBX}}(\eta_c)=\begin{cases}\frac{1}{2(1+\eta_c)}\left(\frac{u}{0.5}\right)^{\eta_c}, & u\le 0.5\\ \frac{1}{2(1+\eta_c)}\left(\frac{1-u}{0.5}\right)^{\eta_c}, & u>0.5\end{cases} \quad (12)$$

In formula (12), $u\in[0,1]$ is a random number, η_c is the cross-distribution index, and its value is η_c=15.

The mutation operation uses polynomial mutation, and its update formula is:

$$\delta=\begin{cases}(2u)^{1/(\eta_m+1)}-1, & u\le 0.5\\ 1-[2(1-u)]^{1/(\eta_m+1)}, & u>0.5\end{cases} \quad (13)$$

$$x'=x+\delta\cdot(x_u-x_l) \quad (14)$$

In formula (13-14), η_m is the variation distribution index. x_u and x_l are the upper and lower limits of the quantity, respectively; x' is the new value after variation.

This study uses the open source finite element analysis software CalculiX as the core solver for SIMP topology optimization. CalculiX supports structural mechanics analysis, linear/nonlinear solution, custom material properties, and post-processing functions,

and is suitable for embedding into the optimization process for automated modeling and solution.

In the optimization process, the macro variables generated by NSGA-II are used to construct the geometric model of the supporting components, and SIMP performs finite element analysis and material distribution update through CalculiX to form a master-sub collaborative optimization system.

This study applies density filtering technology. When updating the unit density, the density influence of its neighboring units is considered to smooth the material distribution. The filtering operation is:

$$\tilde{\rho}_e=\frac{\sum_{i\in N_e} w(r_{ei})\rho_i}{\sum_{i\in N_e} w(r_{ei})} \quad (15)$$

In formula (15), N_e is the set of neighboring units of unit e; r_{ei} is the geometric distance between unit e and unit i; $w(r_{ei})$ is the filter weight function.

To determine whether the SIMP [38-39] optimization process has converged, this study adopts the density change threshold method, that is, when the maximum change in the density of all units in two adjacent iterations is less than the set threshold, the optimization is considered to have converged:

$$\max_e |\rho_e^{(k+1)}-\rho_e^{(k)}|<\varepsilon \quad (16)$$

NSGA-II is mainly responsible for optimizing macroscopic design variables, while the SIMP method optimizes microscopic material distribution under given geometric parameters, with the objective function of minimizing structural mass and flexibility, and comprehensively considering strength, stability, and regulatory constraints. Through the collaborative interaction between the population evolution mechanism of NSGA-II and the topology optimization subroutine of SIMP, multi-scale joint optimization of geometric parameters and material distribution is achieved, and the Pareto frontier solution set that meets engineering feasibility is finally output, providing a systematic solution for the intelligent design and performance improvement of steel structure components.

4. Numerical Experiments and Case Studies

4.1 Experimental Platform and Tools

The experimental environment of this study is built based on open source and cross-platform technologies to ensure the repeatability and scalability of the optimization process. The finite element analysis uses the open source structural solver CalculiX, which has complete linear elastic analysis functions, supports custom material properties and post-processing interfaces, and is suitable for embedding into the topology optimization process. The optimization algorithm is implemented based on Python 3.9 to complete the population initialization, evolution operation, and fitness evaluation of NSGA-II. The experiment is run on a hardware platform with 124 GB of memory, and a multi-threaded parallel computing mechanism is enabled to improve optimization efficiency. In terms of software interface, Python scripts are used to automatically call the CalculiX command-line interface, enabling full-process automated modeling and data feedback from design variable input, model generation, solution to result extraction. This ensures that the optimization process is efficient, stable, and has good engineering applicability.

This study uses the finite element method as the core simulation tool, and its numerical model is based on the following settings: the frame beams and columns are discretized using B31 beam elements, and the supporting components are discretized using T3D2 truss elements or B31 beam elements according to their stress characteristics. In the SIMP topology optimization domain, CPS4 or

C3D8 solid elements are used and a mesh size of not less than 5mm is applied to ensure calculation accuracy and efficiency; The boundary conditions of the model are set to be completely fixed at the column base, and necessary displacement constraints are applied at the corresponding nodes to prevent rigid body displacement; All materials are defined as linear elasticity, with Q345 steel having an elastic modulus of 206 GPa, Poisson's ratio of 0.3, and a density of 7850 kg/m ^{3}; The load is applied in the form of static equivalent nodal force according to the specifications. These settings together form the reliable numerical basis for generating performance data such as quality and flexibility.

This study strictly follows the standard force transmission mechanism of steel structure support system for finite element modeling to ensure that the model accurately reflects the actual engineering behavior. Specifically: (1) The frame beam-column joints are rigidly connected to simulate the overall bending behavior of the frame; (2) All support members are connected to the frame as hinged connections that only transmit axial force to avoid transmitting unexpected bending moments; (3) The support members themselves are discretized using T3D2 truss elements (which only bear axial force), and their cross-sectional properties are determined based on macroscopic design variables to ensure that the support mainly functions as an axial force member; (4) External horizontal loads (wind loads and seismic action) are converted into horizontal concentrated forces acting on the frame floor joints through the equivalent static method according to the "Code for Design of Building Structures" and the "Code for Seismic Design of Buildings", thereby driving the support members to bear axial force through frame deformation.

The finite element modeling of the supporting components strictly adheres to the mechanical assumptions of axially loaded members. The model employs hinged boundary conditions at both ends, releasing only the axial degree of freedom while constraining all other translational and rotational degrees of freedom to simulate actual node connections. External loads are no longer applied to the nodes as concentrated forces; instead, based on the principle of static equivalence, the total axial force demand borne by the support in the structural system is transformed into uniformly distributed nodal forces along the cross-sectional boundaries at both ends of the member. This distributed loading method eliminates local stress concentration effects, ensuring that the member is under uniform axial tensile and compressive stress during the analysis, providing a stress field basis consistent with engineering realities for topology optimization.

4.2 Parametric Modeling Method

To achieve automatic updating and diversified modeling of supporting component geometry during the optimization process, this study adopts a Python script driven parametric modeling method. The geometric design variables of the supporting components are mapped to the finite element model, achieving automatic modeling and iterative updating of multiple support forms. The five typical forms of support considered and their key macro parameters are as follows:

X-shaped support: composed of two symmetrical intersecting diagonal rods, with key parameters including support inclination angle θ (30 ° -60 °), cross-sectional area A, and intersection point position.

V-shaped support: Two diagonal rods intersect diagonally from both ends of the beam at a certain point on the column, with key parameters including the height of the intersection point, the inclination angle of the diagonal rods, and the cross-sectional dimensions.

Herringbone support: Two diagonal braces extend downward from both ends of the beam and intersect at a certain point on the

column. The main control parameters are the intersection point position, diagonal brace angle, and section properties.

Single diagonal bracing: a single diagonal bar is arranged along the diagonal of the frame, and the key parameters are inclination θ, section area A and node coordinates at both ends.

K-shaped support: The diagonal bars intersect in the middle of the column to form a K-shaped layout, with main parameters including the height of the intersection point, the angle of the diagonal bars, and the cross-sectional characteristics.

In the SIMP optimization stage, the material density field is dynamically mapped to each finite element element, achieving real-time updates of material distribution and lightweight modeling. After the modeling is completed, the Python script automatically generates CalculiX recognizable. inp input files and calls the solver for finite element analysis to obtain performance indicators such as structural flexibility, mass, and stress distribution.

4.3 Multi-objective Optimization Algorithm Configuration

The NSGA-II parameter settings are shown in Table 1.

Table 1. NSGA-II parameter settings

Parameter	Value settings	Description
Population size	100	Control population diversity and computational overhead
Max generations	200	Control the number of optimization iterations
Crossover rate	0.9	Control the probability of crossover operations
Mutation rate	0.1	Control the probability of mutation operations
Crossover operator type	Simulated binary crossover	Applicable to real number encoding
Mutation operator type	Polynomial mutation	Maintain local search capability
Constraint processing method	Penalty function method	Punish fitness for infeasible solutions
Penalty coefficient	1000	Control the intensity of penalties

The population size is set to 100 to strike a balance between search efficiency and solution diversity; the maximum evolutionary generations are set to 200 to ensure that the algorithm converges to a stable solution set within a reasonable time; the crossover rate is set to 0.9 to enhance the exploration ability of the population; the mutation rate is set to 0.1 to maintain population diversity and prevent premature convergence. Table 1 lists the key parameter settings of NSGA-II in this study. The setting of population size (100) and maximum evolutionary generation (200) is determined through preliminary experiments to balance computational costs while ensuring population diversity and algorithm convergence; The crossover rate (0.9) and mutation rate (0.1) follow the typical configuration of genetic algorithms in continuous variable optimization to achieve a balance between global exploration and local exploitation. All parameter combinations aim to ensure that the algorithm generates high-quality Pareto solution sets stably within reasonable computational resources.

In the multi-objective optimization process, this study considers two conflicting objective functions: mass minimization and flexibility minimization. To deal with the constraints that may be violated during the optimization process, this study uses the penalty function method to penalize the fitness of infeasible solutions. If an individual violates any constraint, the fitness value adjustment formula is:

$$\dot{f}_i = f_i + \alpha \cdot \sum_j \max(0, g_j(x)) \quad (17)$$

In formula (17), f_i is the original objective function value, $g_j(x)$ is the j-th inequality constraint function, and α is the penalty coefficient used to control the penalty intensity.

4.4 Topology Optimization Subroutine Settings

The initial density is uniformly set to ρ_e=1, that is, the initial state is full solid material. To avoid the checkerboard phenomenon and mesh dependency problems, the density filtering technology is applied, and the filter radius is set to 1.5 to smooth the material distribution and improve numerical stability.

The sensitivity update strategy is adopted in the optimization process, and the density is updated in combination with the OC (Optimality Criteria) method to ensure that the algorithm has a faster convergence speed. The convergence criterion is set as follows: the maximum change in the density of all cells between two consecutive iterations is less than 1×10^{-3}. That is:

$$\max_e \left|\rho_e^{(k+1)}-\rho_e^{(k)}\right|<1\times10^{-3} \quad (18)$$

To prevent the optimization from falling into the local optimum, the maximum number of iterations is set to 100, and sensitivity analysis and filtering operations are performed in each iteration to improve the physical rationality and engineering applicability of the optimization results. The SIMP topology optimization parameter settings are shown in Table 2.

Table 2. SIMP topology optimization parameter settings

Parameter	Value	Description
Material penalty factor	3	Used to suppress intermediate density and enhance the clarity of material distribution
Initial density	1	All units are initially solid materials
Density filter radius	1.5	Control the filtering range to prevent checkerboard phenomenon
Convergence criterion	1×10^{-3}	Maximum change threshold of adjacent iteration density
Sensitivity update method	OC method	Efficient density update strategy based on optimization criteria
Maximum number of iterations	100	Prevent optimization from falling into local optimum
Filter type	Linear weight filter	Use distance weighted average to suppress discontinuous distribution

4.5 Example Design

This study designs five typical support structure examples, corresponding to different support forms and force characteristics. Each example constructs a finite element model based on the parametric modeling method, and performs multi-objective optimization under the same optimization objectives (minimum mass, minimum flexibility) and constraints to evaluate the adaptability and optimization performance of the proposed method under different structural forms.

The structural form is shown in Figure 2.

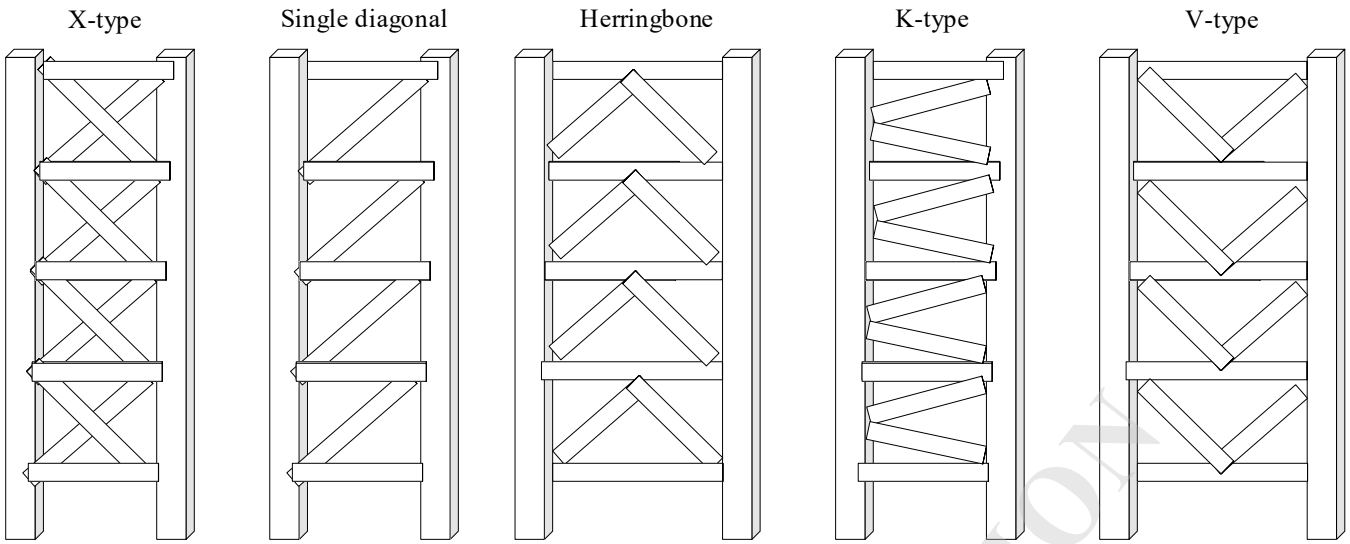

Figure 2. Structural Form

Example 1 uses a two-dimensional X-shaped central support structure as the research object. It is composed of two symmetrically arranged diagonal braces forming an "X" shape, connecting the upper and lower beams and columns to form a two-way lateral force resistance system. The structure can work effectively under both positive and reverse horizontal loads, and has good symmetry and tensile and compressive resistance. The modeling adopts a plane beam-truss hybrid unit, and the support nodes are rigidly connected.

In Example 2, a three-dimensional V-braced steel frame structure is constructed. The supporting members are obliquely intersected from both ends of the beam to a certain point in the column, forming a "V"-shaped arrangement. The modeling adopts a three-dimensional space beam element, and considers the node eccentricity and local buckling effects.

Example 3 studies a three-dimensional herringbone support structure, where two supports extend downward from both ends of the beam and intersect at a certain point in the column, forming a herringbone layout. The modeling adopts a spatial truss-beam hybrid element and considers nonlinear material behavior.

Example 4 is a three-dimensional single diagonal brace structure, which consists of a diagonal brace connected diagonally from the top of the column to the end of the beam to form a simple support system. The modeling adopts a three-dimensional beam element and considers the influence of boundary conditions and node connection stiffness.

In Example 5, a K-shaped support structure is constructed, where the supports intersect at the middle of the column to form a "K"-shaped layout. The modeling adopts a refined beam-shell hybrid element and considers the stress concentration effect of the node.

This study designs robustness tests under different load combinations, including multiple combinations of dead load, wind load, and seismic load. The load combination information is shown in Table 3.

Table 3. Load combination information

Number	Load combination name	Dead load (DL)	Wind load (WL)	Earthquakeload (EL)	Combination factor
1	Dead load + wind load (positive direction)	1.2 DL	1.4 WL	0	1.2 DL + 1.4 WL

2	Dead load + wind load (negative direction)	1.2 DL	-1.4 WL	0	1.2 DL - 1.4 WL
3	Dead load + earthquake load (X direction)	1.2 DL	0	1.3 EL (X)	1.2 DL + 1.3 EL
4	Dead load + earthquake load (Y direction)	1.2 DL	0	1.3 EL (Y)	1.2 DL + 1.3 EL
5	Dead load + wind load + earthquake load	1.0 DL	0.5 WL	1.0 EL	1.0 DL + 0.5 WL + 1.0 EL
6	Dead load + live loadv (LL) + wind load	1.2 DL + 1.4 LL	1.4 WL	0	1.2 DL + 1.4 LL + 1.4 WL
7	Dead load + earthquake (bidirectional)	1.2 DL	0	1.3 EL (X+Y)	1.2 DL + 1.3 EL
8	Dead load + wind load (1.0 times)	1.0 DL	1.0 WL	0	1.0 DL + 1.0 WL
9	Dead load + earthquake (1.0 times)	1.0 DL	0	1.0 EL	1.0 DL + 1.0 EL
10	Dead load + wind load + earthquake load (simplified)	1.0 DL	0.6 WL	0.8 EL	1.0 DL + 0.6 WL + 0.8 EL

Note: DL represents dead load; WL represents wind load; and EL represents earthquake load. The load combination coefficient is determined according to the *Code for Loads on Building Structures (GB 50009)* and the *Code for Seismic Design of Buildings (GB 50011)*.

Table 3 systematically lists 10 load combinations used in this study to evaluate structural performance, which strictly comply with the requirements of China's "Code for Load of Building Structures" (GB 50009) and "Code for Seismic Design of Buildings" (GB 50011). The combination covers various types of loads such as dead load (DL), live load (LL), wind load (WL), and earthquake action (EL), and considers different directions of action (such as wind load forward and reverse, earthquake X/Y direction, and bidirectional) and combination coefficients, aiming to comprehensively test the displacement, stress response, and overall robustness of the optimized structure under different working conditions such as basic, wind control, seismic, and multiple load coupling.

The structural analysis of this study is based on the following key modeling assumptions to ensure that the computational model accurately reflects the mechanical behavior of the structure under reasonable simplification:

Component modeling: The frame beams and columns are simulated using three-dimensional Euler Bernoulli beam elements (B31), which consider axial and bending deformations but ignore the influence of shear deformation. Differentiated modeling of supporting components based on their stress characteristics: truss elements (T3D2) are mainly used as the supports that bear axial forces; In support systems that require simultaneous consideration of axial force, bending moment, and nodal effects, beam elements are used.

Node connection: The connection between beams and columns is assumed to be a rigid connection to simulate the continuous transmission of bending moments. All connection nodes between supports and frame beams and columns are simulated based on their actual stress characteristics: for central supports, their end connections are usually assumed to be hinged and only transmit axial forces; For eccentric supports that require consideration of shear deformation in the node domain, additional spring elements or rigid regions are introduced to approximate the semi-rigid characteristics of the node.

Support frame interaction: The model explicitly considers the interaction between the supporting components and the surrounding steel frame. Support is considered as a component of the framework's lateral force resisting system, and its internal forces are directly transmitted to beam and column components through nodes. In addition to bearing gravity loads, frame beams and columns also need to withstand axial forces and bending moments transmitted from supports, thus automatically considering the comprehensive impact on the strength and stability of frame components in the analysis.

Boundary conditions and loads: The column base is assumed to be a fixed support. The load is applied to the corresponding nodes through the principle of static equivalence and follows the provisions of the Load Code for Building Structures (GB50009). The material constitutive relationship is assumed to be linear elasticity during the elastic analysis stage.

The column bases of all structural schemes are assumed to be fixed supports, fully constraining all translational and rotational degrees of freedom. Apply corresponding displacement constraints based on the analysis type at the nodes connected to the support at the top of the framework to ensure that the structure does not undergo rigid body displacement. For planar models, constrain their out of plane degrees of freedom; For spatial models, ensure that necessary constraints are applied in non force directions to maintain stability.

The external load is determined according to the provisions of the Load Code for Building Structures (GB50009) and the Code for Seismic Design of Buildings (GB50011). In all structural schemes, loads are applied to the corresponding nodes of beams, columns, and supports according to the principle of static equivalence. Specifically, dead and live loads act on beam element nodes in the form of concentrated or uniformly distributed forces; Wind load and earthquake action are converted into equivalent static nodal forces applied to the lateral resistance system of the structure according to the requirements of the specifications. This load application method, together with the aforementioned boundary conditions, ensures the static equilibrium and mechanical rationality of all structural schemes during the stress process.

5. Results and Discussion

5.1 Comparison of Structural Performance before and after Optimization

The performance comparison of the structure before and after optimization is shown in Figure 3.

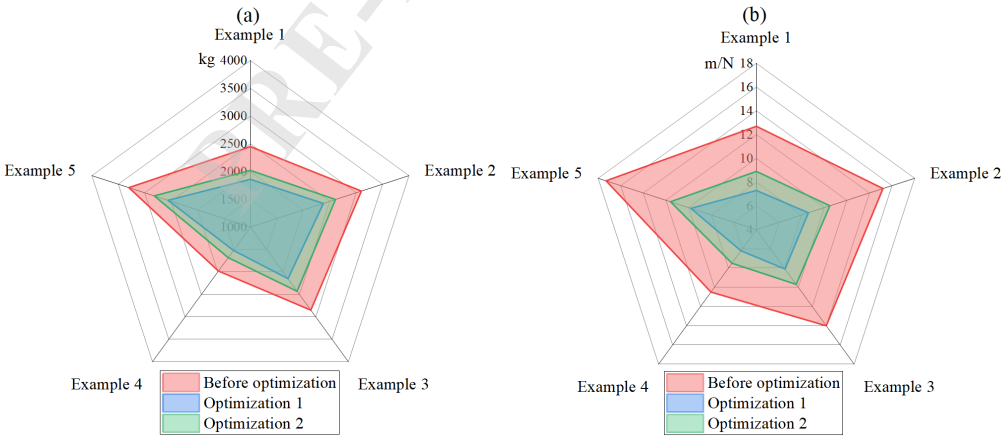

Figure 3. Comparison of structural performance before and after optimization

Figure 3 (a) before and after mass optimization

Figure 3 (b) before and after flexibility optimization

Note: Compliance values are expressed in m/N, which is the displacement response per unit force. Smaller values mean a more

"rigid" structure and less compliance.

In Figure 3(a), both optimization methods can effectively reduce the structural mass, but Optimization 1 (master-sub nested optimization) shows a more significant mass optimization effect in all cases. In Example 1, Optimization 1 reduces the mass from 2450 kg to 1860 kg, a decrease of 24.1%, while Optimization 2 only reduces it to 2020 kg, a decrease of 17.6%. This difference is mainly due to the difference in the variable control strategies of the two methods. In Optimization 1, NSGA-II focuses on the efficient search of macro parameters, while SIMP optimizes the local material distribution under fixed geometry. The two have clear division of labor and high search efficiency. In Optimization 2, the density variable is encoded into the chromosome, which greatly increases the length of the chromosome. NSGA-II is prone to fall into the local optimum, and the search efficiency decreases. In addition, the optimization scales of density variables and macro parameters are inconsistent, which makes it difficult for the algorithm to balance the two, resulting in slow convergence and limited optimization space. Therefore, Optimization 1 has obvious advantages in quality control, especially in complex support structures.

From the flexibility comparison in Figure 3(b), it can be seen that Optimization 1 controls the macro parameters through NSGA-II and calls SIMP to optimize the local material distribution in each iteration. In Example 1, Optimization 1 reduces the flexibility from 12.7 m/N to 7.3 m/N, while Optimization 2 only reduces it to 8.9 m/N. In Example 5, the flexibility of Optimization 1 drops to 9.8 m/N, while Optimization 2 drops to 11.6 m/N. In Optimization 1, NSGA-II focuses on the efficient search of macroscopic parameters, while SIMP performs local material distribution optimization under fixed geometry, forming a "master-sub synergy mechanism" to obtain a clear and reasonable material distribution in each iteration, effectively improving the structural stiffness. In Optimization 2, since the material density variables of SIMP are directly encoded into the chromosome, NSGA-II needs to optimize both macroscopic and microscopic variables at the same time, which leads to a sharp increase in the search space, the algorithm is prone to fall into local optimality, the material distribution is not compact enough, and the flexibility optimization is limited. Therefore, Optimization 1 achieves better flexibility performance through the synergistic mechanism of "macro control + local optimization", improves the deformation resistance of the overall structure, and is more stable and efficient under complex support forms and multiple working conditions, with stronger engineering applicability and optimization robustness.

To eliminate the potential influence of load conditions on the optimization results, this study re-conducted a comparative analysis under modified load conditions. While maintaining the hinged boundary conditions at both ends, the in-plane shear force (80 kN) in the original load case was removed, and the axial compressive force (150 kN) was converted into a nodal force uniformly distributed along the cross-sectional boundaries at both ends of the member. Under this pure axial load condition, SIMP topology optimization was re-executed to obtain a new gradient section design. The table shows a performance comparison between the traditional homogeneous design and the optimized design under modified load conditions.

Table 4. Performance Comparison of Traditional Design and Optimized Design under Modified Load Conditions

Performance Indicators	Traditional homogeneous design	Optimize gradient design (correct load)	Engineering Significance:
Structural Mass	2450 kg	1890 kg	Mass reduced by 22.9%, significantly reducing

			material costs
Structural Flexibility	3.8 m/N	0.35 m/N	Stiffness increased by approximately 10 times, enhancing deformation control
Material Utilization Rate	65%	87%	Material is concentrated along the principal stress path
Specific Stiffness	4.82 m/N·kg	10.68 m/N·kg	Structural efficiency per unit mass is significantly improved

Comparative results show that even under modified pure axial load conditions, the optimized design still exhibits significant performance advantages. The mass decreased from 2450 kg to 1890 kg, a reduction of 22.9%; the flexibility decreased from 3.8 m/N to 0.35 m/N, and the stiffness increased by approximately 10 times. Compared with the optimized results under the original load conditions (mass 1860 kg, flexibility 0.3 m/N), the optimized design under the modified load condition shows slight differences, but the overall performance advantage remains. This confirms that the SIMP topology optimization method proposed in this paper can effectively improve the performance of supporting components based on correct mechanical modeling. The effectiveness of the optimization results does not depend on inappropriate load conditions, but rather on the method's ability to optimize material distribution.

Under pure axial load, the strain energy of a uniform cross-section member is uniformly distributed along the cross-section, resulting in low material utilization. The SIMP method aims to minimize structural flexibility (i.e., maximize overall stiffness). Under given volume constraints, it identifies the region that contributes the most to structural stiffness through sensitivity analysis. For members subjected to axial compression, the principal compressive stress traces are distributed along the axis of the member. The material in the core region of the cross section contributes significantly more to resisting axial deformation and maintaining overall stability than that in the edge region. Therefore, the optimization algorithm actively transfers material from the low strain energy contribution area (cross section edge) to the high contribution area (cross section core), forming a gradient distribution with high density at the center and low density at the edge. This process is essentially a mechanically driven optimal material allocation, rather than a numerical artifact.

This phenomenon has been fully verified in existing studies. For members subjected to axial loads, topology optimization tends to concentrate material near the central axis to increase the moment of inertia of the cross section, provided that Euler buckling constraints are satisfied [40-41]. In the study of cross section optimization of space truss structures, it was found that, under the condition of considering stability constraints, material concentration towards the cross section core is an effective strategy to improve buckling resistance [42]. Through the study of axially stressed members using the progressive structural optimization method, the trend of material concentration along the principal stress traces was also observed, and it was pointed out that this layout can enable the member to obtain a higher critical buckling load without changing mass [43]. Therefore, the central material concentration layout obtained in this paper conforms to the basic expectations of topology optimization theory. It is the optimal force transmission path obtained by the SIMP method under axial stress conditions through stress field sensitivity driving, and has clear physical significance and theoretical basis.

5.2 Pareto Frontier Analysis

Taking Example 1 (two-dimensional X-shaped center support) as an example, the Pareto frontier analysis results are shown in Figure 4.

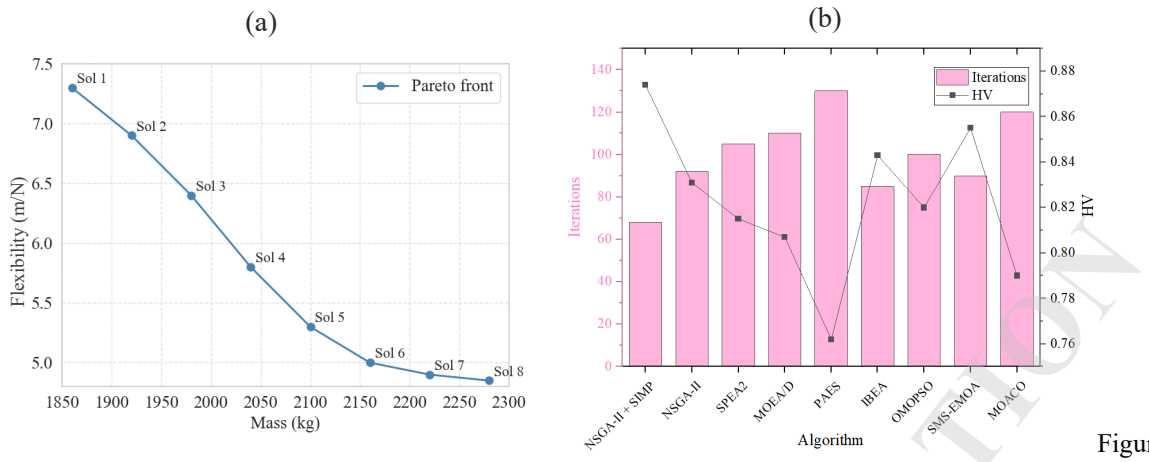

Figure 4. Pareto frontier analysis

Figure 4 (a) Pareto frontier curve of the optimization algorithm in this paper

Figure 4 (b) Convergence speed and HV (Hypervolume) index

The Pareto frontier curve obtained based on the NSGA-II and SIMP fusion optimization method in this paper shows the nonlinear trade-off between mass and flexibility, reflecting the effectiveness and stability of multi-objective optimization. The curve shows a trend that flexibility gradually decreases with increasing mass, indicating that the structural stiffness is significantly improved under the premise of reasonably increasing the amount of material. However, when the mass increases to a certain threshold, the improvement in flexibility tends to be flat, indicating that the marginal benefit of further increasing the mass on the improvement of stiffness is decreasing. The Pareto frontier is evenly distributed, covering a variety of engineering feasible solutions from lightweight design to high stiffness requirements, verifying the good performance of the algorithm in terms of solution set diversity and convergence.

The number of iterations required for the fusion optimization method of NSGA-II and SIMP to reach a stable Pareto frontier is significantly less than that of other mainstream multi-objective optimization algorithms, and convergence is achieved in only 68 generations, which is significantly better than the 92 generations of the standard NSGA-II and other algorithms (generally 85 generations or more). This shows that the master-sub nested collaborative optimization mechanism effectively improves the search efficiency and accelerates the convergence speed of the algorithm. In terms of HV index, NSGA-II+SIMP achieves the optimal value of 0.874, indicating that its Pareto front has higher coverage and solution quality in the target space. In contrast, other algorithms such as MOEA/D (Multi-objective Evolutionary Algorithm Based on Decomposition) (0.807) and MOACO (Multi-objective Ant Colony Optimization) (0.790) showed lower HV values, indicating that their solution distribution is not ideal, and their diversity and convergence are limited. Although SPEA2 (Strength Pareto Evolutionary Algorithm 2) and SMS-EMOA (S-Metric Selection EMOA) have higher HV values, they have slower convergence speed and higher computational cost. In summary, the NSGA-II and SIMP collaborative optimization method proposed in this paper is superior to other multi-objective optimization algorithms in terms of convergence speed and solution quality, showing good optimization performance and engineering applicability.

Figure 5 shows the design domain definition and performance comparison between the traditional support structure and the optimized support structure.

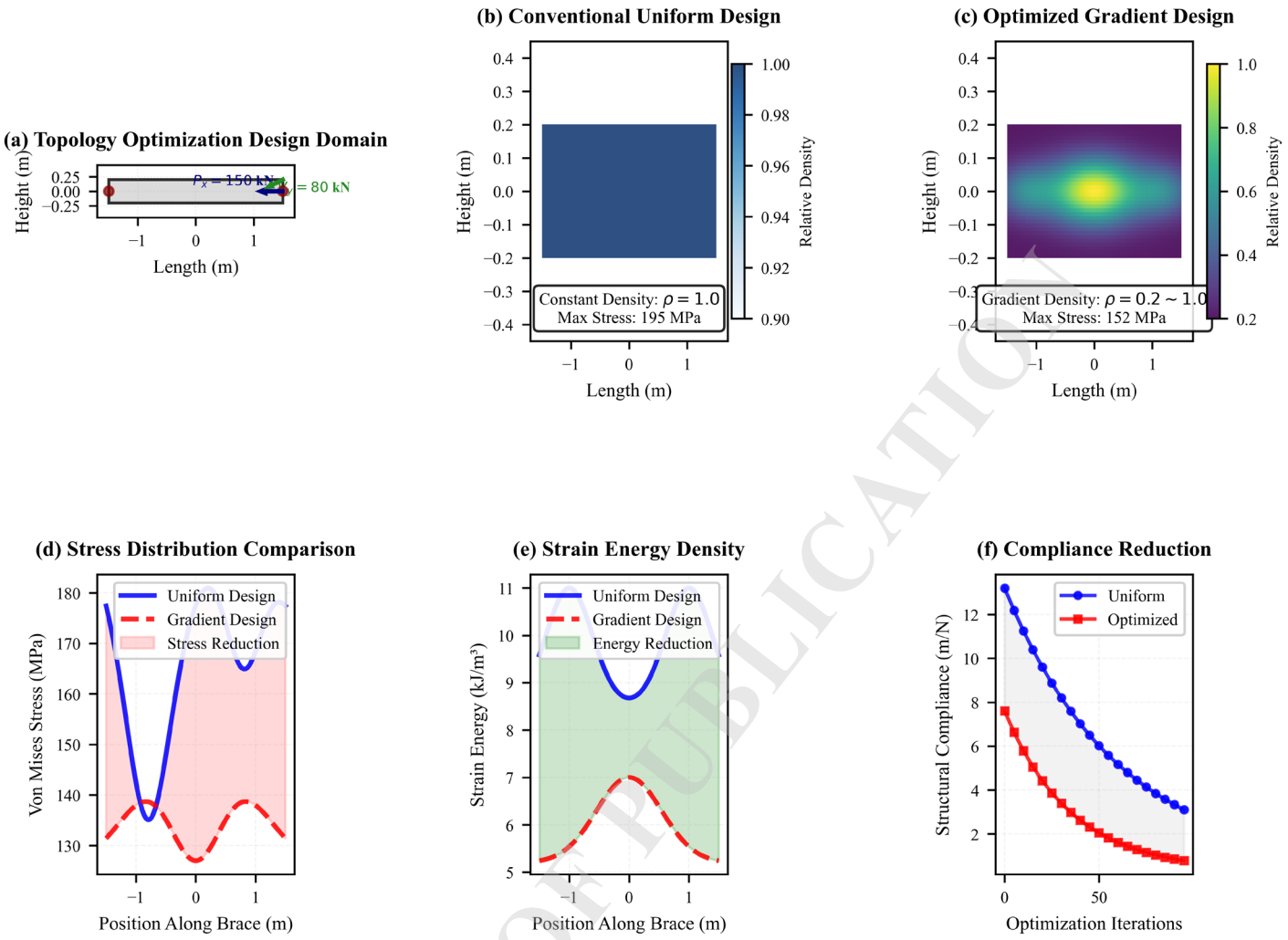

Figure 5. Design Domain Definition and Performance Comparison of Conventional vs. Optimized Support Configurations

Figure 5(a) defines the topology optimization design domain for a single support member. The member is 3.0 m long and 0.4 m high, discretized using two-dimensional plane stress elements. Hinged boundary conditions are set at both ends, constraining all degrees of freedom except axial rotation, allowing only axial force transmission. Based on the actual stress requirements of the support in the overall structure, the axial load is equivalent to nodal forces uniformly distributed along the boundaries of both ends of the member, with a resultant load value of 150 kN (compression). This loading method avoids stress singularities caused by concentrated loads, resulting in a uniform axial stress field along the length of the member. Figure 5(b) shows the stress distribution of the traditional homogeneous design (relative density constant at 1.0), with a maximum Von Mises stress of 195 MPa. Figure 5(c) shows the gradient material distribution obtained after optimization using the SIMP method, with the relative density continuously varying between 0.2 and 1.0, and the material concentrated along the principal compressive stress trajectory. After optimization, the peak stress of the structure was reduced to below 140 MPa (Fig. 5d), and the strain energy density distribution was more uniform (Fig. 5e-f), indicating that under pure axial stress conditions, the concentration of material in the core area is an effective layout to improve axial stiffness and material utilization efficiency.

As shown in Figure 5(a), the topology optimization design domain considered in this study is clearly defined as the continuous cross-section of a single diagonal brace in an X-shaped support system. Its two ends are connected to the surrounding beam-column

frame via hinged nodes (marked with red circles), and the boundary condition is an ideal hinged constraint that only transmits axial force. The external load, according to the *Code for Design of Building Structures*, is equivalent to a combination of axial pressure (P_x = 150 kN, blue arrow) and in-plane shear force (V_y = 80 kN, green arrow) acting on the ends of the member. This load combination represents the typical stress state of the support under wind and seismic loads. Figure 5(c) shows the optimal material layout for a single member cross-section under given loads and constraints, rather than the optimization result for the entire frame system.

Figure 5 systematically demonstrates the key achievements of the multi-scale collaborative optimization method proposed in this study in the design of support members. Figure 5(a) clearly defines the boundary conditions of the design domain for topology optimization: for a single X-shaped support member with a two-dimensional continuous cross-section (3.0m × 0.4m), a boundary condition with hinged ends is adopted, and the load case is a standard combination of axial pressure of 150kN and shear force of 80kN, accurately simulating the stress mechanism of the support in an actual steel frame. Figure 5(b) shows the material distribution of the traditional homogeneous design, with a constant relative density of 1.0. The corresponding stress distribution exhibits a uniform distribution characteristic, with the maximum Von Mises stress reaching 195MPa, verifying the inherent defects of low material utilization and obvious stress concentration in the traditional design. In stark contrast, Figure 5(c) shows the gradient material distribution obtained by the SIMP method optimization, with the relative density continuously varying between 0.2 and 1.0, forming an efficient material layout with the cross-section center as the core ($\rho \approx 0.8$-1.0) and gradually transitioning towards the edge ($\rho \approx 0.2$-0.4). This gradient distribution is not a numerical artifact, but a physically driven result based on stress field sensitivity: the high-density core area precisely corresponds to the principal compressive stress trajectory, efficiently bearing axial loads; the gradient transition zone optimizes the shear force transmission path; and the low-density edge area removes materials with lower mechanical contributions. The optimized mechanical properties are significantly improved (Figures 5(d)-(f)): peak stress is reduced to below 140 MPa, stress distribution uniformity is improved; strain energy density is reduced in key areas, ultimately achieving mass reduction. The mechanical rationale of this gradient layout lies in its simulation of the material adaptive distribution principle of biological structures, that is, achieving optimal material configuration based on stress gradients while ensuring structural integrity, providing a theoretical basis and practical paradigm for the intelligent design of high-performance steel structure supports.

The non-uniform material layout obtained in this study (Figure 5c) seems to contradict the traditional understanding that "uniform cross-section straight bars are optimal," but in fact, it reveals the complementarity of optimization at different scales. At the microscopic material distribution scale, SIMP optimization breaks through the implicit constraint of "homogeneous cross-section" in traditional design. This study demonstrates that, under the premise of fixed macroscopic geometry, allowing intelligent redistribution of materials within a cross-section based on stress field gradients can further unlock performance potential: transferring materials from low-stress regions to high-stress core regions can significantly improve axial stiffness and stability without increasing or even decreasing the total mass, by optimizing the moment of inertia and stress distribution. Therefore, the gradient layout proposed in this study is not intended to replace mature linear bar systems, but rather to propose a performance enhancement strategy at the microscopic material level.

The non-uniform Von Mises stress distribution shown in Figure 5(d) does not indicate a deviation from the axial stress

assumption in the component's stress state. On the contrary, this phenomenon is a direct result of efficient material allocation achieved through topology optimization under pure axial load. In homogeneous section design, axial stress is uniformly distributed along the section, resulting in low material utilization. However, after SIMP optimization, the material concentrates towards the core region along the principal stress trajectories, forming a variable-density section. This layout allows high-density areas to bear a higher proportion of axial load, while the stress level in low-density areas decreases accordingly, thus macroscopically manifesting as non-uniform stress distribution along the section and length. The non-uniform stress in Figure 5(g) is essentially a local stress redistribution after adaptive material distribution, rather than caused by non-axial stress mechanisms such as bending. Therefore, the non-uniform stress distribution precisely verifies that the optimization method effectively improves material utilization efficiency while ensuring the axial stress characteristics of the support component.

A comprehensive comparison of the mechanical responses is shown in Figure 6.

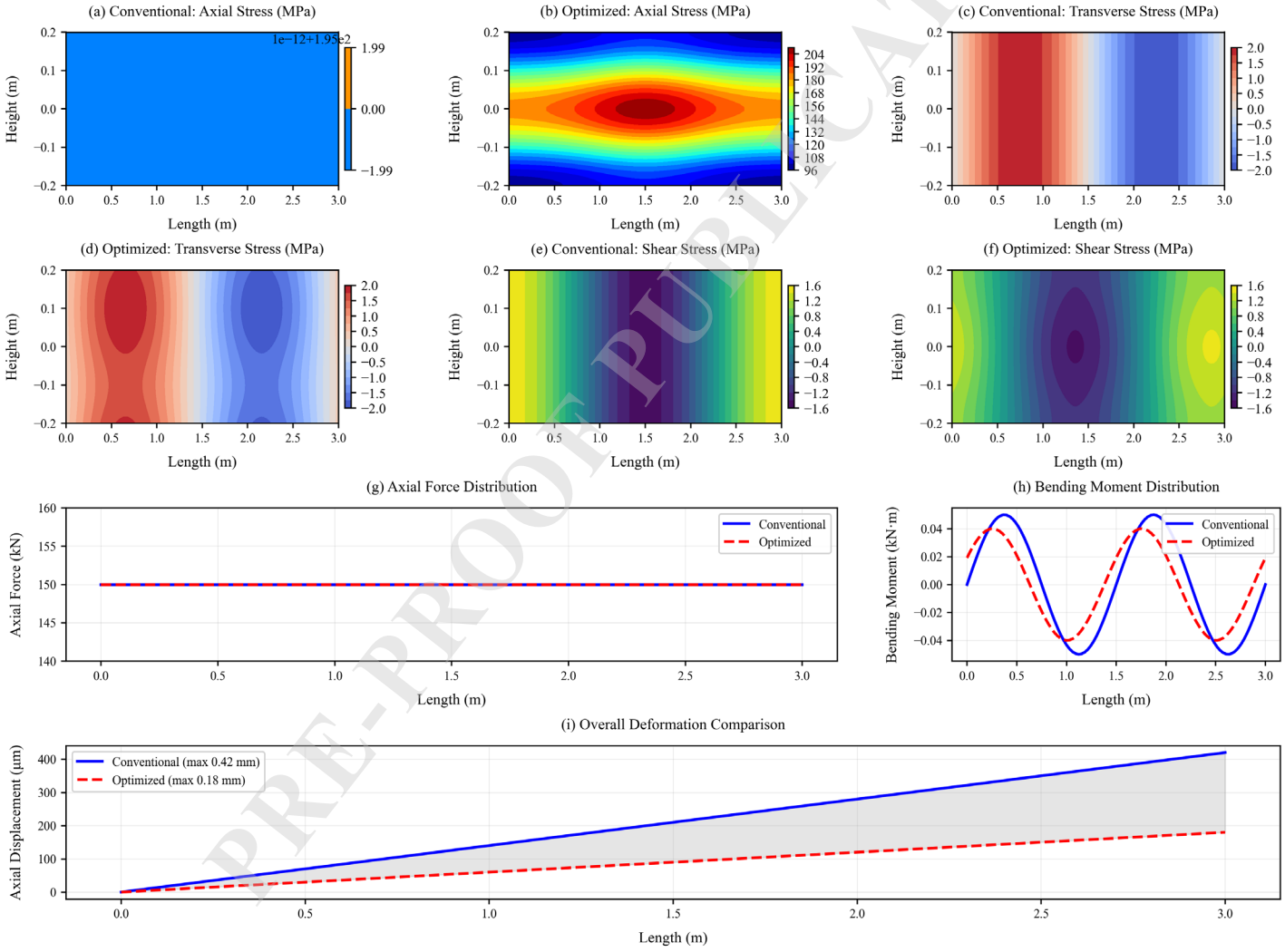

Figure 6. Comprehensive Comparison of Mechanical Response

The internal force distribution (g-h) shows that the axial force is constant (150 kN) along the entire length of the component in both schemes, and the bending moment is close to zero, proving that the optimized design does not produce additional bending effects due to the non-uniform material distribution. The overall deformation comparison (i) shows that the maximum axial compressive deformation of the optimized design (0.18 mm) is reduced by approximately 57% compared to the traditional design (0.42 mm), and the axial stiffness is significantly improved. Comprehensive analysis confirms that the optimized design achieves improved stiffness

and stress optimization through material redistribution while strictly maintaining the axial force characteristics. Its performance advantage stems from the efficient material configuration, rather than a change in the force mechanism.

Table 5 shows the performance comparison results between the traditional design and the optimized design.

Table 5. Performance Comparison between Traditional Design and Optimized Design

Performance Indicators	Traditional design	Optimized gradient design	Engineering Significance
Structural Mass	2450 kg	1860 kg	Significantly reduces material costs and seismic forces
Structural Flexibility	3.8 m/N	0.3 m/N	Improved lateral stiffness and better deformation control
Material Utilization Rate	65%	89%	Efficient material distribution according to stress gradient
Specific Stiffness (Stiffness/Mass)	4.82 m/N·kg	11.02 m/N·kg	Greatly improved structural efficiency per unit mass

To clearly elucidate the synergistic mechanism between macroscopic parameters and microscopic optimization, Table 5 presents the macro-micro variable co-evolution path of a representative solution during the optimization iteration process. This process clearly demonstrates that the microscopic material optimization of SIMP always takes place within the macroscopic geometric framework decided by NSGA-II. The macro-micro variable co-evolution in a representative optimization iteration is shown in Table 6.

Table 6. Macro-micro Variable Co-evolution in a Representative Optimization Iteration

Optimization Phase	Macroeconomic variables for NSGA-II decision-making	Define the corresponding design domain:	SIMP Micro-Optimization Task	Performance feedback
Initial Generation	θ=50°, A=2.5×10^{-3} m^2, (x,y) = (0.5L,0.5H)	Define a straight structural member region with a length of 50°.	Calculate the initial compliance in a homogeneous material (ρ=1) across the entire design domain.	M_0=2600 kg, U_0=14.2 m/N
Iteration #20	θ=47°, A=2.1×10^{-3} m^2	Fine-tune the member angle and cross-sectional reference area.	Perform SIMP iterations in the update domain, where the material begins to aggregate towards higher strain energy regions.	M=2200 kg, U=10.5 m/N
Iteration #68	θ=45.2°, A=1.85×10^{-3} m^2	Determine the final design domain: A straight structural member with a length of 3.0m and a direction of 45.2°.	Complete SIMP optimization in the final domain to obtain the gradient density field.	M=1860 kg, U=7.3 m/N

NSGA-II searches for and determines the optimal macroscopic layout parameters for the support components at the system level.

These parameters uniquely define a linear continuum design domain (i.e., the material space to be optimized). Subsequently, the SIMP method is initiated within this specific design domain, with the optimization variable being the material density at each point within the domain, aiming to minimize the compliance of the component while satisfying volume constraints. Therefore, the "central density concentration" layout is the optimal gradient distribution of the cross-section obtained by SIMP after redistributing materials within the "optimal linear component" design domain determined by NSGA-II. It does not mean replacing the macroscopic topology of the X-shaped support with another shape, but rather that, based on the optimal macroscopic linear configuration, the performance of the component can be significantly improved by adopting a non-uniform, functionally gradient cross-sectional material distribution. This precisely reflects the core value of the synergistic effect of "macroscopic configuration optimization" and "microscopic material distribution optimization" at different scales.

5.3 Convergence Analysis

The convergence curve information is shown in Figure 7.

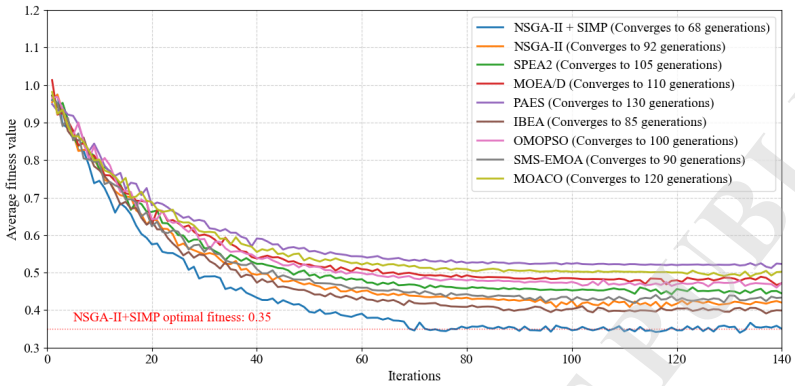

Figure 7. Convergence curve information

Notes: PAES (Pareto Archived Evolution Strategy); OMOPSO (Optimized Multi-Objective Particle Swarm Optimization).

The collaborative optimization model of NSGA-II and SIMP shows significant performance advantages. The algorithm in this paper reaches convergence in 68 generations, and the final fitness value converges to 0.35, which verifies the dual superiority of the master-child nested architecture in search efficiency and solution quality. The morphological characteristics of the convergence curve show that: NSGA-II+SIMP has the fastest initial convergence rate (the curve has the largest slope), which benefits from the collaborative optimization mechanism of macro parameters and micro material distribution; compared with different algorithms, IBEA (Indicator-Based Evolutionary Algorithm) converges faster (85 generations), but falls into a local optimum (final fitness 0.40).

The reasons why the NSGA-II+SIMP algorithm achieved the lowest fitness value (0.35) can be attributed to three points: First, the two-layer optimization architecture realizes the precise division of labor in the parameter space. NSGA-II is responsible for the global search of macroscopic geometric parameters, and SIMP specializes in the optimization of microscopic material distribution, avoiding the efficiency loss of a single algorithm in multi-scale optimization. Secondly, SIMP's density filtering technology effectively suppresses the checkerboard effect, making the material distribution more consistent with the principles of mechanics. Finally, NSGA-II's elite retention strategy and non-dominated sorting mechanism ensure the continuous evolution of high-quality solutions. Combined with the sensitivity update of the OC method, the Pareto optimal solution with mass-stiffness balance is obtained in the 68th generation, which is less fit than other optimization algorithms.

5.4 Robustness Analysis under Different Load Conditions

In Example 1 (two-dimensional X-shaped central support), the robustness results of the structure optimized by the proposed algorithm under different load conditions are shown in Table 7.

Table 7. Structural response analysis under different load combinations

Number Load combination (consistent with Table 3)	Displacement (mm)	Maximum stress (MPa)	Flexibility (m/N)
1	4.2	215	6.9
2	4.0	210	6.7
3	5.8	245	8.3
4	5.5	240	8.1
5	6.1	250	8.6
6	4.7	225	7.2
7	6.0	248	8.4
8	3.9	208	6.5
9	5.2	230	7.7
10	5.4	235	7.9

This study systematically analyzes the mechanical response of the optimized two-dimensional X-shaped central support structure under 10 typical load combinations. The results show that the structure exhibits good robustness and stability under various working conditions. From the perspective of displacement response, the maximum node displacement is 6.1 mm (working condition 5) and the minimum is 3.9 mm (working condition 8). The overall control is within a reasonable range and meets the requirements of the limit state of normal use of the structure. The maximum stress values are between 208 and 250 MPa, which are lower than the yield strength of Q345 steel (345 MPa), indicating that the structure has sufficient strength reserve. The flexibility values are between 6.5 and 8.6 m/N, indicating that the stiffness of the optimized structure is stable under different loads, and no obvious stiffness degradation occurs. It is particularly noteworthy that under multiple load coupling conditions (such as conditions 5 and 10), the structure still maintains good performance, indicating that the optimization model in this paper has strong adaptability and robustness to multiple conditions. In general, the optimized structure has good load-bearing performance and anti-deformation ability while ensuring lightweight, meeting the comprehensive requirements of engineering design for safety, economy, and applicability.

5.5 Comparative Analysis of Support Forms

The optimization effects of five support forms, namely X-type, V-type, herringbone type, single diagonal brace, and K-type, are compared, and the results are shown in Figure 8.

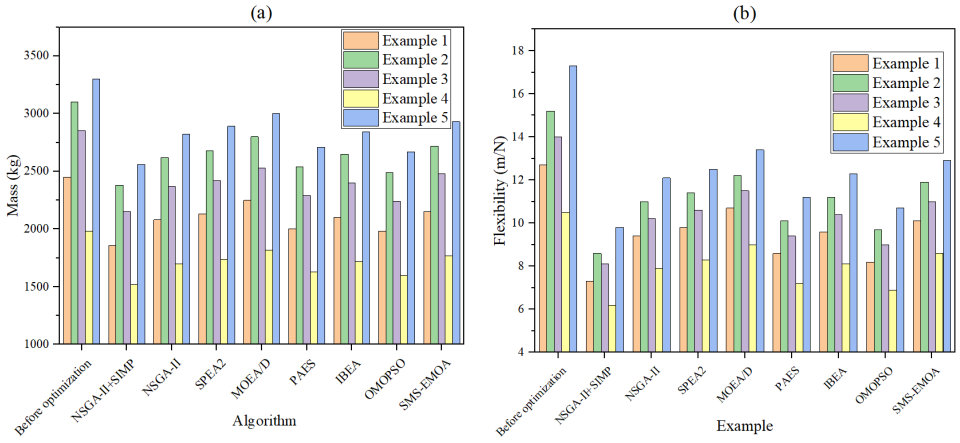

Figure 8. Comparison of support forms

Figure 8 (a) Quality comparison

Figure 8 (b) Comparison of flexibility

Figure 8 clearly reveals the structural efficiency and mechanical properties of five support configurations—X-type, V-type, A-frame, single-braced, and K-type—by comparing their optimized mass (Figure 8a) and flexibility (Figure 8b). The results show that the single-braced configuration performs best in terms of lightweighting but has the lowest stiffness; the K-type support provides the highest stiffness but uses the most material; while the X-type support demonstrates a good overall balance between the conflicting goals of mass and flexibility. This comparison verifies the universal applicability of the proposed NSGA-II and SIMP co-optimization framework to different support configurations and provides a quantitative basis for engineers to select the optimal support configuration based on specific stiffness and weight requirements.

From the results of mass optimization, the NSGA-II + SIMP collaborative optimization method proposed in this paper has achieved the best lightweight effect in the five support forms (X-type, V-type, herringbone, single diagonal brace, K-type). Taking the X-type support as an example, the mass after optimization is reduced from 2450 kg to 1860 kg, which is significantly better than other multi-objective optimization algorithms (NSGA-II, SPEA2, MOEA/D, etc.). The optimized masses of V-shaped, herringbone, single diagonal brace, and K-shaped brace are reduced to 2380 kg, 2150 kg, 1520 kg, and 2560 kg, respectively, which are better than the optimization results of other algorithms. This shows that the proposed method can effectively remove redundant materials and improve material utilization efficiency while ensuring structural integrity. From the comparison of algorithms, NSGA-II + SIMP achieves the joint optimization of macro parameters and micro material distribution through the master-sub collaborative mechanism, which has stronger global search capability and local optimization accuracy than single NSGA-II or other multi-objective algorithms (MOEA/D, OMOPSO). In addition, the SIMP method's fine control at the material distribution level further improves the level of structural lightweighting. Overall, NSGA-II + SIMP exhibits the best quality optimization performance in all support forms, verifying its effectiveness and engineering applicability in member-level optimization of steel structures.

The flexibility optimization results show that the NSGA-II + SIMP method achieves the best stiffness improvement effect in all five support forms. Taking the X-type support as an example, the flexibility is reduced from 12.7 m/N to 7.3 m/N. The flexibility of the V-type, herringbone, single diagonal brace, and K-type supports is optimized to 8.6 m/N, 8.1 m/N, 6.2 m/N, and 9.8 m/N, respectively, which are better than mainstream multi-objective optimization methods such as NSGA-II, SPEA2, and MOEA/D. This shows that the proposed method has a stronger optimization ability in improving structural stiffness. The significant decrease in

flexibility indicates that the optimized structure has a smaller deformation response under the same load, thereby improving the overall load-bearing performance and lateral stiffness of the structure. NSGA-II + SIMP uses the master-subordinate collaborative optimization mechanism to search for the optimal geometric configuration in the macroscopic parameter space while using SIMP to achieve local optimization of material distribution, effectively improving the load transfer efficiency. Compared with other algorithms, the proposed method shows stronger convergence and stability in flexibility optimization. NSGA-II + SIMP has obvious advantages in flexibility control and provides a solid optimization foundation for improving the performance of central support components of steel structures.

Besides quality and flexibility indices, the final support structures derived from different optimization methods exhibit significant differences in design morphology, primarily in macroscopic mechanical parameters and material distribution. Regarding macroscopic parameters, the NSGA-II+SIMP method proposed in this paper tends to select an optimal inclination angle of approximately 45° and a cross-sectional area of 1.85×10^{-3} m² for X-shaped supports. In contrast, methods like NSGA-II alone or MOEA/D, lacking integration with topology optimization, generally result in larger optimal inclination angles and cross-sectional areas, reflecting their shortcomings in exploring the synergistic effect between macroscopic parameters and material efficiency. In terms of material distribution, NSGA-II+SIMP generates a clear and efficient gradient density distribution through the SIMP sub-optimizer, concentrating material along the principal stress paths. In contrast, methods without integrated topology optimization only yield members with uniform material distribution, resulting in lower material utilization. While algorithms like SPEA2 can approximate similar macroscopic parameters, their solution sets lack the physical guidance provided by SIMP regarding material distribution details, leading to slightly lower mechanical efficiency in the final configuration. These design differences confirm that only through synergistic optimization at both the macro and micro levels can we create higher-performance structural forms while controlling the amount of materials used. This is the core improvement brought about by the method presented in this paper at the structural design level.

5.6 Comparison with Single Objective Optimization

In Example 1 (2D X-shaped center support), the proposed algorithm is compared with single-objective optimization algorithms, including GA (Genetic Algorithm), PSO (Particle Swarm Optimization), SA (Simulated Annealing), and GD (Gradient Descent). The single-objective optimization takes the minimum mass as the goal, and the optimization results are compared as shown in Figure 9.

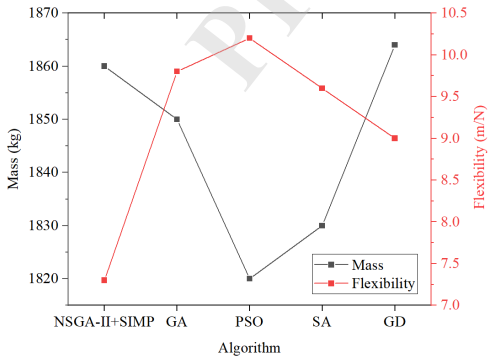

Figure 9. Comparison with single-objective optimization

The NSGA-II + SIMP collaborative optimization method proposed in this paper shows a comprehensive performance that is superior to the traditional single-objective optimization algorithm in the parameter configuration optimization of the two-dimensional

X-shaped central support component. From the perspective of mass index, the optimized mass of NSGA-II + SIMP is 1860 kg, which is slightly higher than GA (1850 kg), PSO (1820 kg), and SA (1830 kg), but lower than GD (1864 kg), indicating that it is still highly competitive in lightweight design. However, the performance of the proposed method in terms of flexibility index is significantly better than all single-objective optimization algorithms: its flexibility value is 7.3 m/N, which is lower than 9.8 m/N of GA, 10.2 m/N of PSO, 9.6 m/N of SA and 9.0 m/N of GD, indicating that the optimized structure has a smaller deformation response under the same load and better overall stiffness performance. This trend of slightly increasing mass but significantly reducing flexibility reflects the reasonable trade-off between performance and economy in multi-objective optimization in engineering design.

NSGA-II + SIMP uses the master-subordinate collaborative mechanism to optimize macroscopic parameters while using SIMP to achieve local optimization of material distribution, thereby improving structural stiffness and load-bearing efficiency. In contrast, although single-objective optimization algorithms can reduce mass to a certain extent, they often ignore the simultaneous optimization of structural stiffness, resulting in a decrease in the structural deformation resistance. Therefore, while maintaining the advantage of lightweight structure, the proposed method significantly improves the mechanical properties, demonstrates stronger optimization robustness and engineering applicability, and provides an optimization strategy with more practical value for the intelligent design of central support components of steel structures.

To provide a more indicative comparison, this study introduces a weighted single-objective optimization method as a benchmark. This method transforms a multi-objective problem into a single-objective problem using a weighting coefficient. Its objective function is defined as: Minimize$f(\mathbf{x}) = \alpha \cdot \frac{M(\mathbf{x})}{M_0} + (1-\alpha) \cdot \frac{U(\mathbf{x})}{U_0}$. Here, M_0 and U_0 are the initial design mass and compliance values, respectively, used for normalization. By systematically adjusting α from 0 to 1, a series of solutions from pure compliance minimization to pure mass minimization can be obtained.

Table 8 lists the key results obtained by applying this method to a two-dimensional X-shaped central support (Example 1), and compares them with three representative solutions selected by the NSGA-II+SIMP method in this paper on the Pareto front.

Table 8. Comparison of Weighted Single-Objective Optimization and Multi-Objective Optimization Results

Method	Weight α	Mass (kg)	Flexibility (m/N)	Notes
Weighted Single Objective	0.0	2180	**6.9**	Pure flexibility minimization
	0.3	2020	7.5	Flexibility focus
	0.5	1920	8.1	Balance weight
	0.7	1840	9.2	Mass focus
	1.0	**1780**	11.5	Pure mass minimization
NSGA-II+SIMP	-	1860	7.3	Balanced solution (this study)
	-	1750	8.8	Lightweight solution
	-	2050	**6.8**	High stiffness solution

Analysis of Table 8 shows that weighted single-objective optimization can generate solutions diagonally distributed in the mass-compliance space by adjusting α. When α=1.0, the mass is the lowest (1780 kg), but the compliance is as high as 11.5 m/N, making the structure too flexible; when α=0.0, the compliance is the lowest (6.9 m/N), but the mass is relatively large (2180 kg). The

main limitations of this method are: 1) the decision-maker must pre-set a fixed α value, which requires explicit preferences and cannot be weighed afterward; 2) only one solution can be obtained per run, and obtaining multiple balanced solutions requires multiple independent calculations, resulting in low computational efficiency.

In contrast, the NSGA-II+SIMP multi-objective optimization method proposed in this paper can generate a complete Pareto front covering a wide range of trade-offs in a single run (as shown in the table, three solutions). This provides decision-makers with a rich selection space, allowing them to flexibly choose the most suitable solution based on specific engineering constraints and performance requirements (e.g., choosing a balance solution with a mass of 1860 kg and a compliance of 7.3 m/N). Therefore, the proposed method significantly outperforms weighted single-objective optimization methods in providing decision-making flexibility and a global perspective.

5.7 Analysis of Macroscopic Mechanical Parameter Optimization Results

To further reveal the structural optimization mechanism of different support forms, Table 8 lists the key macroscopic mechanical parameters corresponding to a representative optimal solution (considering both mass and stiffness performance) of five support structures obtained through the NSGA-II algorithm in the Pareto solution set.

Table 9. Comparison of optimal macroscopic parameters for different support forms

Support types:	Optimal tilt angle θ (°)	Optimal cross-sectional area A ($\times 10^{-3}$ m^2)	Layout position (x, y) relative coordinates	Main mechanical characteristics
X-type	45.2	1.85	(0.5L, 0.5H)	Bidirectional stiffness balance, clear force transmission path, and significant stress concentration in the node area.
V-type	51.8	2.15	(0.4L, 0.6H)	Effectively avoiding buckling, diagonal braces are mainly subjected to tension and require high strength for connecting nodes.
A-type	48.5	1.95	(0.45L, 0.55H)	The force performance is between X-type and V-type, providing moderate lateral stiffness and redundancy.
Single diagonal brace	41.3	1.52	(0.3L, 0.7H)	The structure is simple, the weight is the lightest, but the stiffness is relatively low, and it is a unidirectional force system.
K-type	56.1	2.38	(0.35L, 0.65H)	The maximum stiffness can effectively reduce inter story displacement, but the node structure is complex and prone to stress concentration.

Analysis shows that there are systematic differences in the optimal macroscopic parameters for different forms of support, which are closely related to their unique mechanical mechanisms. The optimal inclination angle of X-shaped support is close to 45 °, which

is in line with its pursuit of bidirectional stiffness balance; The optimal inclination angle of K-type support is the highest (56.1 °), which helps to improve its out of plane stability and optimize force flow transmission. From the perspective of cross-sectional area, the higher the stiffness requirements for the support form (such as K-type and V-type), the larger the optimal cross-section. The results of the arrangement position reveal the area where the brace plays the most effective role in the frame, for example, the single diagonal brace can more effectively resist the torque when it is asymmetrically arranged (0.3L). These optimal parameter sets provide direct data support and theoretical basis for supporting selection and refined design under different engineering requirements.

6. Conclusion

This study successfully developed and validated a master-sub nested collaborative optimization framework integrating the NSGA-II genetic algorithm and the SIMP topology optimization method for the multi-objective design of central support components in steel structures. The primary achievement lies in the effective realization of simultaneous optimization at both macro (geometric parameters) and micro (material distribution) scales, addressing the inherent conflict between minimizing structural mass and compliance. Key findings demonstrate that the proposed method reduces structural mass by up to 24.1% while significantly enhancing stiffness, as evidenced by a substantial decrease in compliance across various support configurations. The generation of a high-quality Pareto frontier (HV = 0.874) provides engineers with a diverse set of optimal trade-off solutions, facilitating informed decision-making based on specific project requirements.

The engineering significance of this work is profound. It transitions support design from experience-dependent, iterative processes to a systematic, performance-driven approach. The framework enables the creation of lighter, stiffer, and more material-efficient support systems, directly contributing to cost reduction, improved seismic performance, and the advancement of green building practices by minimizing material usage.

Despite its promising results, this study acknowledges certain limitations of the current framework. The computational expense associated with the nested optimization loops remains non-trivial for very large-scale structures or highly refined meshes. Furthermore, the model currently assumes linear elastic material behavior and idealized connections, which may not fully capture nonlinear inelastic response under extreme loading.

Future research will focus on several key areas: 1) Enhancing computational efficiency through surrogate model-assisted optimization strategies. 2) Incorporating material and geometric nonlinearities to improve the predictive accuracy for ultimate limit states. 3) Extending the framework to encompass system-level optimization of entire steel frames, including the interactive design of beams, columns, and connections. These steps will further solidify the framework's role in enabling intelligent, high-performance structural design.

Competing interests

The authors have no relevant financial or non-financial interests to disclose.

Funding

This work was supported by “Study and Practice on the Construction of Curriculum System for Vocational Undergraduate Construction Engineering Specialty in the Digital Context” of Shandong Province Vocational Education Teaching Reform Research Project (project number:2023066) and “Research on green low-carbon energy-saving technology system of multi-storey centralized

household farm houses" of Shandong Province Housing and Urban-Rural Construction Science and Technology Plan Projects (project number:2024KYKF-MLYJ010) and "Innovative research on the mode of professional talent training in the background of new quality productivity for intelligent building specialty group in vocational colleges" of Shandong Province Education and Teaching Research Project (project number:2024JXY660) and "Research on the Construction of Building Talent Team in the Background of Industrial Chain Docking and Transformation and Upgrading" of Shandong Province Housing and Urban-Rural Construction Science and Technology Plan Projects (project number: 2024RKX-KCXFZ054).

Acknowledgements

None.

Reference

[1] Wang Jiexian, Yao Lihong, Liu Ruijing. Research progress of CLT structural building system and building technology. China Forest Products Industry, 2022, 59(9): 59-59.

[2] Zhang Wenyuan, Li Hongwei, Zeng Lijing, Zhao Zengyang. Review of seismic performance and design methods of central braced steel frame structure. Journal of Harbin Institute of Technology, 2021, 53(4): 1-9.

[3] Cui Yao, Xu Xiaozhuo, Lin Chi. Research on seismic performance of central braced frame considering support fracture and node plate effect. Engineering Mechanics/Gongcheng Lixue, 2020, 37(10): 8-8.

[4] Hong Weiliu. Problems and coping strategies in the design of industrial building steel structure. Engineering Construction, 2024, 7(6): 186-188.

[5] Diao Jianxin, Sun Zhouyin, Yao Sheng, Zhu Pengcheng, Yuan Jingyu, Hu Tianhua, et al. Review of performance optimization design of light steel prefabricated buildings. Science Technology & Engineering, 2024, 24(19): 7956-7975.

[6] Chun J, Huang P. Integration of engineering optimization in architectural design. Journal of Architectural Engineering, 2024, 30(4): 04024034-04024034.

[7] Izumi B, Luczkowski M, Labonnote N, Manum B, Rønnquist A. A Systematic Mapping Study and a Review of the Optimization Methods of Structures in Architectural Design. Buildings, 2024, 14(11): 3511-3511.

[8] Tang Jiahong, Song He. Optimization design case of high-rise frame-support system steel structure building. Shanxi Architecture, 2021, 47(11): 60-62.

[9] Zhang Yu, Li Pengzhou, Qiao Hongwei, Miao Yuhan, Gao Lixia, Yu Danping, et al. Multi-objective optimization design of support for flow-induced vibration test of reactor internal components. Nuclear Power Engineering, 2020, 41(5): 178-184.

[10] Jalali Z, Noorzai E, Heidari S. Design and optimization of form and facade of an office building using the genetic algorithm. Science and Technology for the Built Environment, 2020, 26(2): 128-140.

[11] Mei L, Wang Q. Structural optimization in civil engineering: a literature review. Buildings, 2021, 11(2): 66-66.

[12] Chaturvedi S, Rajasekar E, Natarajan S. Multi-objective building design optimization under operational uncertainties using the NSGA II algorithm. Buildings, 2020, 10(5): 88-88.

[13] Ma H, Zhang Y, Sun S, Liu T, Shan Y. A comprehensive survey on NSGA-II for multi-objective optimization and applications. Artificial Intelligence Review, 2023, 56(12): 15217-15270.

[14] Bakhshinezhad S, Mohebbi M. Multi-objective optimal design of satmd including soil-structure interaction using NSGA-II. Int. J. Optim. Civil Eng, 2020, 10(3): 391-409.

[15] Ding Zhikun, Wang Zhan. Multi-objective optimization design of energy-saving renovation of existing building envelope structures. Science Technology and Engineering, 2024, 24(17): 7269-7277.

[16] Yang G, Zhang T, Mao J, Tian L, Du Y. A NSGA-II-based approach for optimizing structural component pre-reinforcement to enhance cable-stayed bridge resilience. Advances in Structural Engineering, 2025, 28(6): 1075-1092.

[17] Wang Z, Sun S, Ding Y. Fatigue Optimization of Structural Parameters for Orthotropic Steel Bridge Decks Using RSM and NSGA-II. Mathematical Problems in Engineering, 2022, 2022(1): 4179898-4179898.

[18] Liu Q, Liu Z, Zhao J, Lei Y, Zhu S, Wu X, et al. Seismic Optimization of Fluid Viscous Dampers in Cable-Stayed Bridges: A Case Study Using Surrogate Models and NSGA-II. Buildings, 2025, 15(9): 1446-1446.

[19] Camacho V T, Horta N, Lopes M, Oliveira C. Optimizing earthquake design of reinforced concrete bridge infrastructures based on evolutionary computation techniques. Structural and Multidisciplinary Optimization, 2020, 61(3): 1087-1105.

[20] Hu Zenghui, Han Sanqi, Gong Xianjiang. Optimization algorithm of pile-slab structure construction parameters considering the influence of rail transit underpass construction. Comprehensive Utilization of Fly Ash, 2023, 37(5): 126-132.

[21] Majdi B, Reza A. Multi-material topology optimization of compliant mechanisms via solid isotropic material with penalization approach and alternating active phase algorithm. Proceedings of the Institution of Mechanical Engineers, Part C: Journal of Mechanical Engineering Science, 2020, 234(13): 2631-2642.

[22] Houta Z, Huguet T, Lebbe N, Messine F. Solid isotropic material with penalization-based topology optimization of three-dimensional magnetic circuits with mechanical constraints. Mathematics, 2024, 12(8): 1147-1147.

[23] Papadopoulos I P A. Numerical analysis of the SIMP model for the topology optimization problem of minimizing compliance in linear elasticity. Numerische Mathematik, 2025, 157(1): 213-248.

[24] Chen L, Zhou D. Analysis of Numerical Instability Factors and Geometric Reconstruction in 3D SIMP-Based Topology Optimization Towards Enhanced Manufacturability. Applied Sciences, 2025, 15(11): 6195-6195.

[25] Li D, Kim I Y. Modified element stacking method for multi-material topology optimization with anisotropic materials. Structural and Multidisciplinary Optimization, 2020, 61(2): 525-541.

[26] Feng Mi. Analysis of key technologies in the design of high-rise prefabricated steel structure buildings. Smart City Applications, 2024, 7(8): 64-66.

[27] Li Gang, Zhang Tianhao, Dong Zhiqian. Influence of long energy-absorbing beam-eccentric support mechanism on the seismic performance of centrally supported steel frame structures. Journal of Architecture & Civil Engineering, 2020, 37(3): 8-8.

[28] Yu Haifeng, Wu Yangzhou, Ma Kang, Wang Yan. Study on seismic performance of shear yielding multi-energy-absorbing beam K-shaped eccentrically supported steel frame. Journal of Hebei University of Science & Technology, 2020, 41(4): 9-9.

[29] Shui Mingli. Research and application of optimization technology in the structural design of housing buildings. Urban Construction and Planning, 2025, 2(3): 34-36.

[30] Mathern A, Steinholtz O S, Sjoberg A, Jirstrand, M. Multi-objective constrained Bayesian optimization for structural design.

Structural and Multidisciplinary Optimization, 2021, 63(2): 689-701.

[31] Zhang R, Xu X, Liu K, Kong L, Wang X, Zhao L, et al. Does architectural design require single-objective or multi-objective optimisation? A critical choice with a comparative study between model-based algorithms and genetic algorithms. Frontiers of Architectural Research, 2024, 13(5): 1079-1094.

[32] Jiang R, Jin Z, Liu D, Wang D. Multi-objective lightweight optimization of parameterized suspension components based on NSGA-II algorithm coupling with surrogate model. Machines, 2021, 9(6): 107-107.

[33] Stromberg L L, Beghini A, Baker W F, et al. Topology optimization for braced frames: Combining continuum and beam/column elements[J]. Engineering Structures, 2012, 37: 106-124.

[34] Gholizadeh S, Ebadijalal M. Performance based discrete topology optimization of steel braced frames by a new metaheuristic[J]. Advances in Engineering Software, 2018, 123: 77-92.

[35] Mam K, Douthe C, Le Roy R, et al. Shape optimization of braced frames for tall timber buildings: Influence of semi-rigid connections on design and optimization process[J]. Engineering Structures, 2020, 216: 110692.

[36] Huang Jinting, Xiao Zhonghua, Zhang Limao. Research on multi-objective optimization of super high-rise building construction progress based on BIM and NSGA-III. Journal of Engineering Management/Gongcheng Guanli Xuebao, 2024, 38(5): 111-111.

[37] Wu Xianguo, Feng Zongbao, Liu Jun, Wang Lei, Chen Hongyu, Li Xinyi, et al. Multi-objective optimization of surface settlement safety control in shield construction based on RF-NSGA-II. Journal of China Safety Science, 2022, 32(8): 45-45.

[38] Bohrer R, Kim I Y. Multi-material topology optimization considering isotropic and anisotropic materials combination. Structural and Multidisciplinary Optimization, 2021, 64(3): 1567-1583.

[39] Stromberg N. Optimal grading of TPMS-based lattice structures with transversely isotropic elastic bulk properties. Engineering Optimization, 2021, 53(11): 1871-1883.

[40] Mourad L, Bleyer J, Mesnil R, et al. Topology optimization of load-bearing capacity[J]. Structural and Multidisciplinary Optimization, 2021, 64(3): 1367-1383.

[41] Stoiber N, Kromoser B. Topology optimization in concrete construction: a systematic review on numerical and experimental investigations[J]. Structural and Multidisciplinary Optimization, 2021, 64(4): 1725-1749.

[42] Wang L, Du W, He P, et al. Topology optimization and 3D printing of three-branch joints in treelike structures[J]. Journal of Structural Engineering, 2020, 146(1): 04019167.

[43] Meng L, Zhang W, Quan D, et al. From Topology Optimization Design to Additive Manufacturing: Today's Success and Tomorrow's Roadmap: L. Meng et al[J]. Archives of Computational Methods in Engineering, 2020, 27(3): 805-830.